An Efficient and Low-Cost Hierarchical FANET Architecture Using the Attached Mobility Model to Create the Core Layer for Connecting UAVs and Ground Control Stations

Tho C. Mai [1,2,*], Ly T. H. Nguyen [2], Cuong Q. Nguyen [1,3], Le Huu Binh [1], and Tu T. Vo [1]

[1] Faculty of Information Technology, Hue University of Sciences, Hue University, Hue City, Vietnam
[2] Faculty of Information Technology, Nha Trang University, Nha Trang City, Vietnam
[3] Faculty of Natural Science and Technology, Tay Nguyen University, Buon Ma Thuot City, Vietnam
Email: mctho@hueuni.edu.vn (T.C.M.); lynth@ntu.edu.vn (L.T.H.N.); nqcuong.dhkh23@hueuni.edu.vn (C.Q.N.); lhbinh@hueuni.edu.vn (L.H.B.); vttu@hueuni.edu.vn (T.T.V.)
*Corresponding author

***Abstract*—Due to the frequent movement of the Unmanned Aerial Vehicles (UAVs) in Flying Ad-Hoc Network (FANET), increasing the Packet Delivery Ratio (PDR) from the UAVs to the Ground Control Station (GCS) is a major problem. In this research, a solution is suggested, which has been enhanced from standard Unmanned aerial Vehicle (UAV) to address this challenge. The idea of the proposed solution is to create a two-layer hierarchical FANET, core and access layers. The core layer consists of several UAVs flying according to the attached mobility model to form a backbone connecting to the GCS. The access layer includes the remaining UAVs that use the core layer UAVs as gateways to transmit data to the GCS. The proposed solution is compared with the improved architecture in term of PDR, throughput, and end-to-end-delay. Simulation results conducted using OMNeT++ demonstrate that the proposed method outperforms the improved architecture in the evaluated performance metrics.**

***Keywords*—Flying Ad-Hoc Network (FANET) architecture, Unmanned Aerial Vehicle (UAV), attached mobility model, end-to-end communications**

I. Introduction

Flying Ad-Hoc Network (FANET) is a type of ad-hoc wireless network composed of a group of Unmanned Aerial Vehicles (UAVs), with at least one of them being connected to a Ground Control Station (GCS) or Satellite. In this network, UAVs communicate and collaborate to transmit data to the GCS while carrying out designated tasks [1, 2]. FANET is a specific instance of a Vehicular Ad-hoc Network (VANET), which, in turn, is a particular case of a Mobile Ad-hoc Network (MANET). Consequently, FANET shares all the attributes inherent to MANET, including self-sufficiency without dependence on fixed network infrastructure, cost-effectiveness, rapid deployment, and extensive mobility. Within the FANET, network nodes engage in mutual communication, effectively functioning as both hosts and routers.

FANET has garnered substantial scholarly interest in recent years due to its potential applicability across various domains, encompassing critical areas such as disaster response, search and rescue missions, environmental monitoring, and military reconnaissance, among others [1, 3, 4] (see Fig. 1).

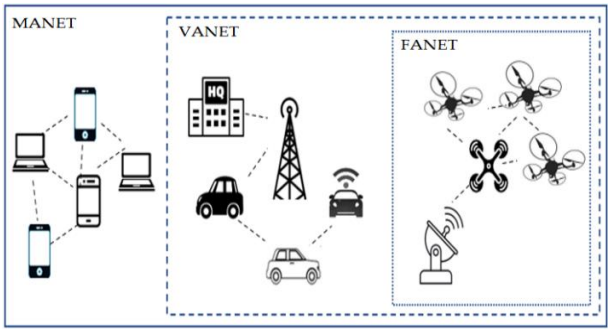

Fig. 1. Some special cases of wireless ad-hoc networks [1].

In the realm of MANET/FANET routing, finding the most efficient data transmission path is more complex than choosing the shortest route in terms of hop count. The shortest path isn't always the best due to frequent link disruptions, instability, and traversing nodes with limited resources. FANET routing research covers various metrics, including packet speed, link stability, quality, load, lifespan, distance, and node energy levels. Strategies for route recovery in case of link failures, like backup routes and error packet propagation, are explored. The routing challenges in FANET have attracted substantial research attention, as seen in dedicated publications [4]. However, achieving end-to-end communication efficiency remains a persistent challenge, requiring ongoing research and development.

Manuscript received August 19, 2023; revised November 1, 2023; accepted November 16, 2023; published April 16, 2024.

Routing protocols, in fact, are part of the network architecture. The network architecture explains how the network is constructed and how nodes communicate with one another, whereas the routing protocol defines how nodes create and maintain routes to transport data on that architecture. It demonstrates that the routing protocol design is also based on a certain FANET architecture, and network performance is likewise influenced by the network architecture. Research on enhancing FANET performance mostly focuses on increasing routing efficiency on FANET by developing new routing protocols [5–9] or improving current MANET routing protocols to be consistent with FANET [10–12]. The authors of the majority of the published results constructed FANET simulation models using the same strategy as MANET, that is, the nodes have the same purpose and use the same mobility model. In fact, in most FANET applications, the objective is to collect data from the environment and relay it to a ground base station. However, research on enhancing FANET performance primarily focuses on the end-to-end communication between UAVs and has not adequately addressed the efficiency of communication between UAVs and GCS. Of course, the GCS can be seen as a UAV, but its properties, such as mobility, processing power, and transmission range, are entirely different from those of UAVs.

Standard UAV ad-hoc network architecture (a type of FANET architecture which will be covered in Session II [2]) exhibit advantageous characteristics in terms of cost-effectiveness, efficiency, and ease of deployment. These networks are economically viable due to their utilization of basic communication protocols, which minimize the need for advanced hardware and software components. Moreover, proximity-based communication enables direct connections between UAVs, resulting in reduced latency and improved overall network efficiency. Additionally, the simplicity of deploying standard UAV ad-hoc networks allows for quick and straightforward implementation in various mission environments. However, it is important to acknowledge that these networks may face challenges related to link quality, network partitioning, and scalability as the number of UAVs increases. The adoption of multi-group and multi-tier architectures [2] addresses certain limitations inherent in the standard architecture, particularly in cases where a homogeneous collection of UAVs is deployed in a FANET. However, it is important to note that the implementation of these architectures is relatively more complex and expensive compared to the standard architecture. The establishment of groups or layers requires additional configuration and coordination, which can be challenging and time-consuming. Moreover, the deployment of specialized hardware and software components may be necessary, increasing the overall cost of the network infrastructure.

A proposed strategy to modify the standard UAV ad-hoc network with the additional use of attached mobility model for exploiting their advantages to help enhance network performance, especially communication efficiency with GCS is our motivation for doing this work.

The following are the primary contributions of this work:

(1) The FANET architecture and its impact on network performance are investigated;

(2) An efficient and cost-effective hierarchical FANET architecture is presented, enhanced from the standard FANET architecture, with the aim of reducing network partitioning, enhancing scalability, stabilizing the route from UAVs to GCS, all of which contribute to enhancing the overall network performance. This approach comprises two layers: The core layer consists of several UAVs flying according to the attached mobility model to form a backbone connecting to the GCS, and the access layer includes the remaining UAVs that use the core layer UAVs as gateways to transmit data to the GCS.

The remainder of the paper is organized as follows. Section II describes related works on FANET performance improvement based on network design improvements. Section III presents our proposed architecture. The experimental results and discussion are presented in Section IV. Finally, concluding remarks and promising future study items are given in Section V.

II. Related Works

As discussed in Section I, network architecture is one of the main factors affecting FANET performance. In this section, the basic FANET architectures and some related works on improving network performance based on this factor are presented.

Li *et al.* [2] proposed four distinct architectures for FANET, namely centralized UAV network, UAV ad-hoc network (Standard UAV ad-hoc network), multi-group UAV ad-hoc network and multi-layer UAV ad-hoc network. In the centralized UAV network, the GCS serves as a central node, establishing direct connections with all UAVs to facilitate data transmission. Fig. 2 illustrates the architecture of UAV ad-hoc network, which incorporates a backbone UAV functioning as a gateway for the ad-hoc network, enabling data transfer between the GCS and other UAVs.

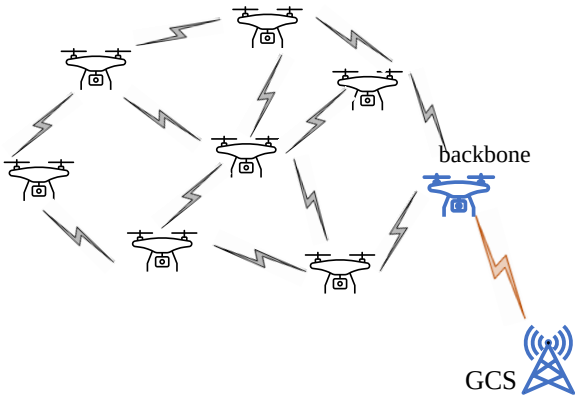

Fig. 2. Illustrate the UAV Ad-hoc network architecture [2].

Utilizing a backbone UAV helps facilitate communication between all UAVs in the network and external entities, extending the effective communication

range of the entire network. This allows UAVs to maintain a connection with the GCS even when they operate beyond the GCS's direct communication range. However, employing a backbone UAV also presents a set of challenges and limitations, including stability issues and the potential risk of it becoming a single point of failure in communication with the GCS or other networks. Standard UAV ad-hoc networks face challenges related to link quality and network partitioning. Proximity-based communication in these networks can result in varying link quality issue, impacting the reliability of communication. Moreover, network partitioning can occur in dynamic or harsh environments, isolating UAVs and hindering information exchange and coordination. Multi-group and multi-layer UAV ad-hoc networks represent advanced variations that enhance the capabilities of standard UAV ad-hoc networks. Standard UAV ad-hoc networks operate as indivisible networks without explicit grouping or layering, relying on proximity-based communication. Conversely, multi-group networks partition UAVs into distinct groups or clusters based on predefined criteria, facilitating focused communication and coordination within each group. Multi-layer networks organize UAVs into hierarchical layers, promoting specialized task execution and efficient resource utilization. Communication within groups or layers occurs more frequently and directly, necessitating relaying or designated gateways for inter-group or inter-layer communication. However, the successful implementation of these advanced network architectures poses challenges related to group or layer formation, inter-group or inter-layer communication, synchronization, and scalability management.

Because the rapidly changing topology in standard UAV ad-hoc network causes ineffective communication between UAVs-UAVs, UAVs-GCS, Kim *et al.* [13] proposed adding more UAVs that are only responsible for data relay. In this suggested architecture, the mission UAVs (mUAVs) conduct their responsibilities and generate data to be relayed to the GCS, while the relay UAVs (rUAVs) are in charge of relaying the data of mUAV to the GCS. With the assumption that the positions of the mUAVs and GCSs are predefined, the authors propose a topology construction and topology correction algorithm to calculate and adjust the suitable positions for the rUAVs to build an efficient FANET providing end-to-end communication between the mUAVs and the GCS. The proposed optimization problem is NP-hard, the Particle Swarm Optimization (PSO) algorithm is used by the author to build the topology. The results of simulation with FANET, which included four mUAVs, one GCS at a fixed position, and more than seven rUAVs, show that the technique produces a good topology that makes end-to-end communication more efficient than random topology (deploying rUAVs in random locations). Due to the fixed position of the mUAVs, the author's simulation is not really ideal for the FANET scenario. When the positions of the mUAVs are constantly or rapidly changing, it is necessary to quickly recalculate the positions of the rUAVs for deployment.

Emphasizing the idea that the position of the relay plays a crucial role in either solving problems or improving network performance, Jaiton *et al.* [14] proposed a novel approach to enhance communication in a FANET using UAV relays through a combination of machine learning and optimization techniques. The primary focus of the approach is to optimize the placement of relays in order to enhance data collection and transmission. This is achieved through the utilization of an Artificial Neural Network (ANN) trained with simulated data. The simulated data includes various factors such as the position of the UAV relay, the positions of UAVs involved in the flight mission, the throughput of each UAV during the mission with the UAV relay, and the Received Signal Strength Indication (RSSI) of each UAV during the mission with the UAV relay. The ANN predicts optimal transmission rates based on UAV and relay positions. A heuristic algorithm, guided by the ANN's output, then determines the new relay UAV position, maximizing data traffic collection.

FANET architecture based on Software Defined Networking (SDN) has also been implemented by several research groups recently. Silva *et al.* [15] presented STFANET, a topology management algorithm for FANET based on the SDN-FANET architecture. The suggested architecture involves a FANET composed of a UAV controller (cnUAV), a set of mUAVs, and a set of rUAVs. cnUAV is primarily in charge of monitoring node positions as well as setting up and managing the complete network. As a result, cUAV changes the routing table of each node (mUAV and rUAV) and determines the location of the rUAVs. Although the cUAV can act as a relay node, it only collects and transmits control packets in order to focus processing power on the dispatch function. cnUAV saves routing and position information for each node in order to administer the network topology. The PSO algorithm is also used by STFANET to create the topology in order to discover the optimal position for the rUAVs and itself. Because of the mobility of the mUAVs, the positions of the cnUAV and the rUAVs are constantly changing, and thus network performance is affected by the processing speed of the cnUAV and the amount of control and location information shared. switch rUAV and cnUAV.

Emadi and Mohannadi [16] proposed an improved network architecture from multi-group UAV ad-hoc network using master Clusters (CH) and Alternate Master Clusters (ACH) to overcome the problem of single point failure and consider the problem of energy efficiency and remaining battery life of the UAV backbone. Each cluster/group in this design assigns CH and ACH based on the node's current state, including battery capacity, signal strength, and remaining power. Each CH acts as a UAV backbone (gateway) responsible for communicating with other group CHs and GCS. After a period, or when the energy of CH falls below a certain threshold, the role of being the gateway is passed to the ACH. When a CH/ACH of UAV is out of range of the GCS, the cluster connection is employed to support communication with the GCS. Using ACH increases network and storage costs. This is due to the fact that the ACH must get the same network updates as the CH in order to be accessible to assume the

job of the CH at any given time. While storage capacity is not an issue for UAVs because recent advancements allow them to be modified with additional storage as needed, network cost remains an issue. The increased amount of information that must be transferred between the UAVs in the cluster to identify the ACH, as well as between the new ACH and the earth station and other CHs, increases network expenses.

In the sphere of FANET routing protocol research, a substantial number of new or enhanced protocols derived from MANET or VANET protocols have been proposed. This has been substantiated by numerous survey and evaluation articles encompassing both FANET and VANET. These articles include Jiang and Han [17], Arafat and Moh [18], Oubbati *et al.* [19], Lakew *et al*. [20], Sang *et al.* [21], Güneş and Abasıkeleş [22], and Wheeb *et al.* [23]. They have jointly synthesized and clarified the strengths and weaknesses of existing routing protocols, grouped according to classifications (topology-based routing, location-based routing, combined topology/ and location routing, etc.) for FANET, VANET, and also point out the formulas and research directions. Each protocol has its own strengths and weaknesses, and no one protocol is suitable for all FANET applications. Their effectiveness also depends on many factors such as mobility model, movement speed, remaining energy, UAV communication technology, FANET architecture, and deployment strategy. Therefore, it can be seen that improving FANET performance solely based on routing protocols is not enough, as they can hardly achieve the same performance as routing protocols for wired networks, wireless sensor networks, or MANET networks.

III. Proposed Architecture

In this section, the proposed architecture is presented, which is an improved version of the standard UAV ad-hoc architecture with the additional use of a attached mobility model.

In the deployment of FANET to encompass a vast area, the transmission route between UAV and GCS often necessitates traversing multiple hops. However, due to the high mobility of UAVs and the sparse distribution of FANET nodes, the hop-by-hop links are prone to frequent disruptions, resulting in route failures and diminished network performance. The proposed strategy aims to improve end-to-GCS communication efficiency by mitigating the occurrence of link failures along the route. By reducing the number of broken links in the transmission path, we seek to optimize the overall network performance and ensure reliable communication between UAVs and GCS.

Fig. 3. An example of data transmission route from S to D, including links L1, L2, L3 and L4.

Fig. 3 depicts a data transmission route from Source (S) to Destination (D) established through four successive hops, consisting of hop-by-hop links L4, L3, L2, and L1. Any of these 4 links is broken resulting in a broken route and needs to be updated again.

Nevertheless, when multiple links are broken simultaneously, the cost of reconstructing the route becomes higher as more links need to be reestablished, the ability to find an alternative route is impacted as the network topology undergoes rapid changes. This leads to reduced network performance.

Under the assumption that link L1 remains unbroken, the probability of the remaining route breaking is 3/4. By additionally ensuring that link L2 remains unbroken, the remaining probability of route breakage reduces to 2/4. Similarly, with the addition of link L3 without encountering any breakages, the remaining probability of route breakage decreases to 1/4. Finally, by guaranteeing the addition of link L4 without any breaks, the possibility of route breakage becomes 0/4, meaning the route remains intact and unbroken. The attached mobility model helps us achieve these assumptions.

Based on the arguments presented above, the following is a description of the proposed architecture.

Fig. 4 illustrates an example of FANET using this architecture. All UAVs in the network are divided into two layers, one used for the core layer which includes the backbone UAVs (BU) and one used for the access UAV (AU).

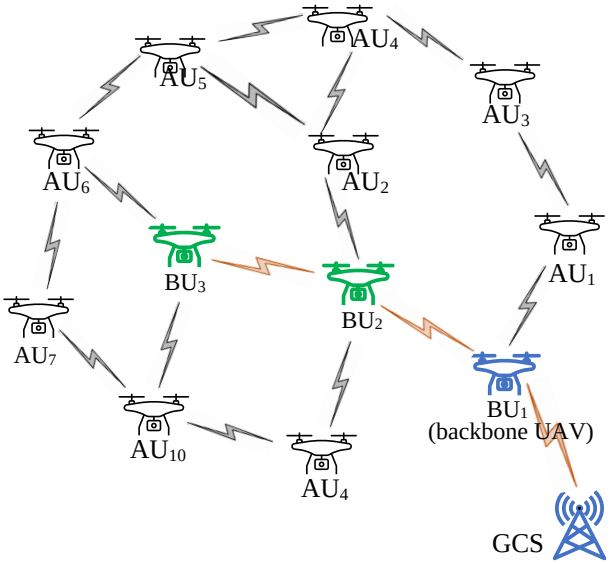

Fig. 4. An example of B-FANET architecture.

To ensure that the BUs constantly maintain a backbone network connected to the GCS, they must move according to the attached mobility model. This mobility model, introduced in INET [24] framework, allows to define the motion of the BUs relative to a reference point which is the GCS in this context. At each instant, every BU has a speed and direction that is derived by from that of the GCS.

The backbone, which is made up of BUs, serves as the expanded communication range of the GCS. As a result, the AUs can easily connect to the GCS through this backbone network. The AUs move according to the popular models of the FANET.

In the case of core layer has only one BU1, this architecture becomes the standard UAV ad-hoc network.

The choice of the number of BUs, the topology of the core layer depends on the number of BUs that can be used, along with the communication range of the BUs, AUs and the FANET deployment area.

In this work, the proposed architecture is implemented with the use of increasing BUs (from one to four BUs) and connecting them in a straight line.

- The UAVs operating in the space bounded by the box are $[0, 0, K\ ]$: $[\ M_x, M_y, M_z]$ (Fig. 5)
- The communication range of the AUs is R_a, of the BUs is R_b $(R_b \geq R_a)$, BU_1 can have a second network interface to communicate with the GCS with the communication range R_s, if BU1 shares a network interface, then $R_s = R_b$
- Given the position of the GCS as $[\ G_x, G_{y_t}, 0\ ]$, assuming the GCS is located to the right of the UAVs workspace: $G_x \geq M_x$, $G_{y_t} \in [0, M_y]$, t means the value may change over time.

The location of the BUs is determined as follows:

Number of BUs that can be used: from 1 to *n*, with:

$$n = \left\lfloor \frac{M_x}{R_b} \right\rfloor \quad (1)$$

To ensure connection of BU_1 with GCS, then $D_s \leq R_s$.

$$\begin{cases} X_{BU_1} = G_x - \Delta_x \\ Y_{BU_1} = G_{y_t} \\ Z_{BU_1} = K + h \end{cases} \quad (2)$$

with $h \in [0, M_z - K]$ and Δ_x adjusted to ensure $D_s = \sqrt{(K+h)^2 - {\Delta_x}^2} \leq R_s$

To ensure connection between other BUs:

$$\forall j \in [2, n], \begin{cases} X_{BU_j} = X_{BU_{j-1}} - R_b \\ Y_{BU_j} = Y_{BU_1} \\ Z_{BUj} = Z_{BU1} \end{cases} \quad (3)$$

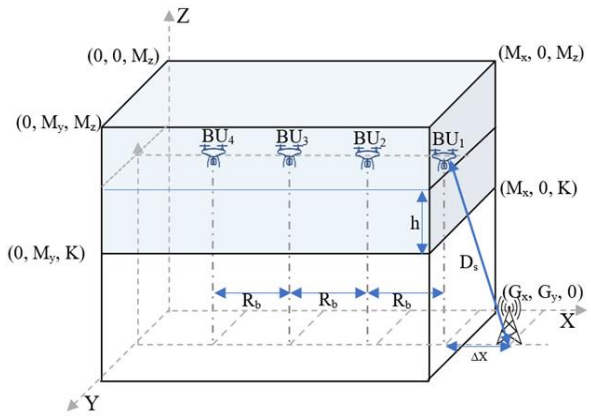

Fig. 5. Illustrate BU positions and other parameters.

The procedure for implementing the proposed architecture is as follows:

Algorithm 1. The process of implementing 2-layer hierarchical FANET architecture

(1) Define FANET deployment space: [M_x, M_y, M_z], where M_x, M_y and M_z are the length, width and height of the network space, respectively;
(2) Determine the coordinates and the mobility model of the GCS;
(3) Calculate the required number of BUs according to (1);
(4) Determine the coordinates of the first BU according to (2);
(5) Determine the coordinates of the remaining BUs according to (3);
(6) Set the mobility model for the BUs to be the Attached Mobility with the reference position being the coordinates of the GCS.
(7) Set the another common mobility model for the AUs;
(8) Set the routing protocol for the BUs and AUs;

IV. Performance Evaluation

A. Simulation Scenario

The performance of the proposed architecture was evaluated via simulation using OMNeT++ and INET framework. The simulation assumptions are listed in Table I The simulation is set up on the area of 1500 × 1500 m^2 with an altitude from 150 to 200 m. Each simulation scenario was run ten times, and the results in this section are the average of those ten runs. The performance of the proposed architecture is compared with that of the standard UAV ad-hoc network architecture (see Fig. 6).

TABLE I. Parameter for Simulation

Parameter	Value
Network Simulator	OMNET++6/ INET4
Mobility Model	Mass Mobility, and Attached Mobility
Routing protocol	AODV
Propagation model	Free Space Path Loss
Simulation area	1500 × 1500 m^2, maximum altitude: 200 m
Simulation time	600 s
Simulation runs	10
Transmission range	250 m
Number of Connection to GCS	10, 20, 30, 40
Number of BU	1, 2, 3, 4
GCS location	Middle, Under, Above, Move

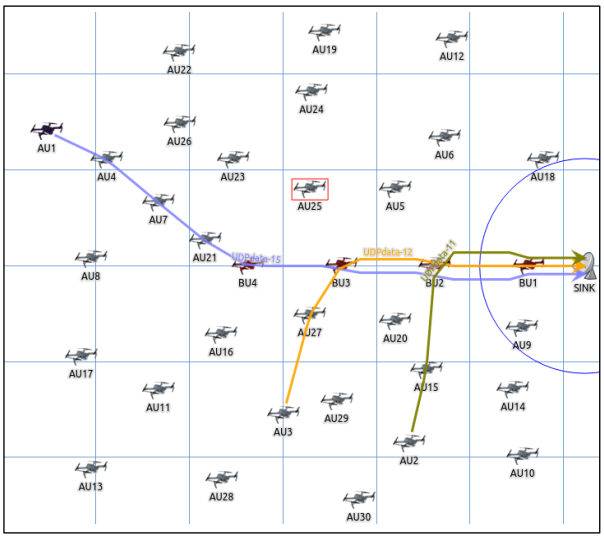

Fig. 6. A topology of the FANET used for simulation.

V. Performance Metrics

In the simulation models, Packet Delivery Ratio (PDR), average end-to-end-delay and network throughput serve as metrics for evaluating and analyzing the performance of proposed architecture.

- PDR is defined as the ratio of the number of the received packets by the destination nodes to the number of sent packets by the source nodes, given by

$$PDR = \frac{\sum packet_{received}}{\sum packet_{sent}} \times 100\%$$

- Average end-to-end delay is defined as the ratio of the number of delays to the number of successfully received packets by the destination node (excluding lost packets), denoted $delay_{avg}$, calculated by

$$Delay_{avg} = \frac{\sum_{i=1}^{n}(t_{receive} - t_{send})}{n}$$

where n is the number of successfully received packets.

- Average throughput is defined as the successfully received data traffic per time unit, determined by

$$Throughput_{avg} = \frac{sizeof(packet) \times \sum packet_{received}}{T}$$

VI. Result and Discussion

A. Effect of Mobility Speed

In this section, the impact of mobility speed of AUs on network performance in terms of PDR, delay-end-to-end and throughput, is investigated. The results obtained in Fig. 7 show the PDR versus the average mobility speed in cases of 50 nodes where each simulation scenario is run 10 times and number of connections to GCS is set at 20. It can be observed that the PDR increases according to the number of BUs for all cases of mobility speed. The higher the mobility speed, the bigger the difference. Considering the case of mobility speed of 25 m/s, the median PDRs for one, two, three, and four BUs are 55.33%, 62.20%, 68.3% and 71.89%, respectively. The relative average PDRs are 55.75%, 62.18%, 68.21%, and 71.78%.

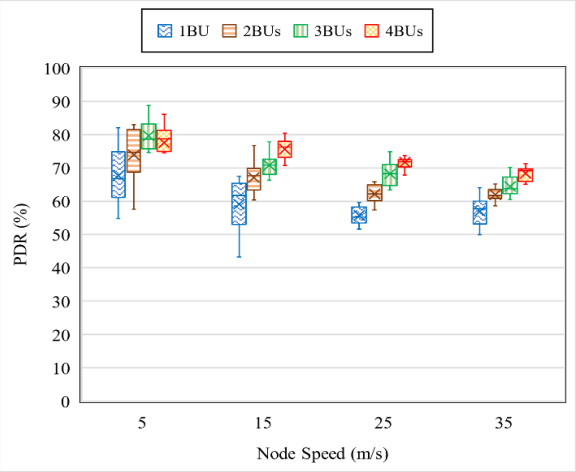

Fig. 7. PDR performance versus mobility speed for simulation scenarios where total BUs differ.

Additionally, Table II supplements the graphical representation, detailing the packet delivery ratio concerning node speed and total BUs. The median and average values across different speeds and BU configurations further underline the direct correlation between increased BUs and enhanced PDR.

TABLE II. Packet Delivery Ratio vs. Node's Speed by Total BUs

Measures	Node speed (m/s)	Packet Delivery Ratio (%)			
		1BU	2BUs	3BUs	4BUs
Median	5	66.85%	74.58%	78.62%	78.70%
	15	61.69%	67.77%	70.90%	76.28%
	25	55.33%	62.20%	68.30%	71.89%
	35	57.78%	61.71%	63.73%	69.14%
Average	5	67.68%	73.91%	79.63%	77.58%
	15	59.13%	67.15%	70.80%	75.63%
	25	55.75%	62.18%	68.21%	71.78%
	35	56.98%	61.96%	64.47%	68.34%

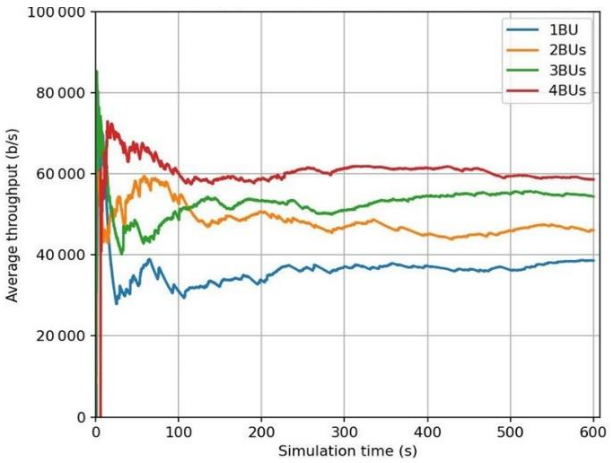

Fig. 8. Throughput performance versus simulation time for scenarios where total BUs differ.

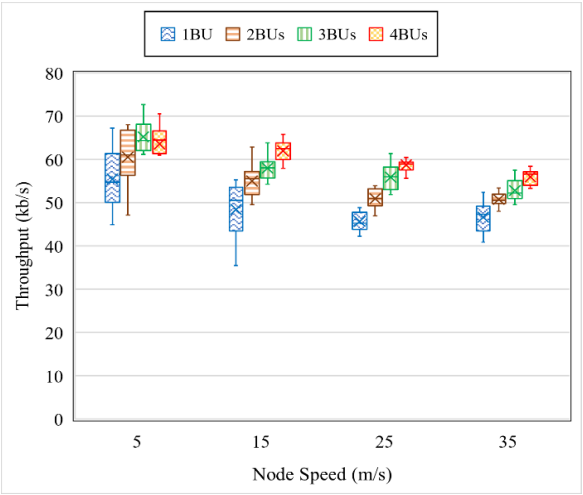

Fig. 9. Throughput performance versus mobility speed for scenarios where total BUs differ.

Because the proposed architecture has a high PDR, the throughput increases as well. Fig. 8 shows the average throughput as a function of simulation time. Observations indicate that when the simulation time is less than 120 s, the throughput fluctuates a lot since the network system is

not stable yet. When the simulation time exceeds 120 s, the average throughput begins to stabilize, with average values of 38.5%, 46.10%, 54.39%, and 58.65% kbps for the one, two, three, and four BUs scenarios, respectively. Thus, throughput increases proportionally to the total number of BUs. This is obvious because when there are more BUs, the coverage of the backbone network is wider. Therefore, the probability that the AU successfully connects to the GCS increases, which in turn increases the network throughput. The effect of mobility speed of nodes on throughput was also investigated with the results obtained as shown in Fig. 9. The box plots in this figure illustrate that the faster the nodes move, the lower the throughput. However, the use case of more BUs always results in higher throughput.

Following that, the end-to-end delay in the entire network is examined. Fig. 10 depicts the latency of data packets versus the mobility speed of nodes, and Table III provides detailed insights. It's evident that the end-to-end delay decreases as the number of BUs increases in most scenarios of mobility speed.

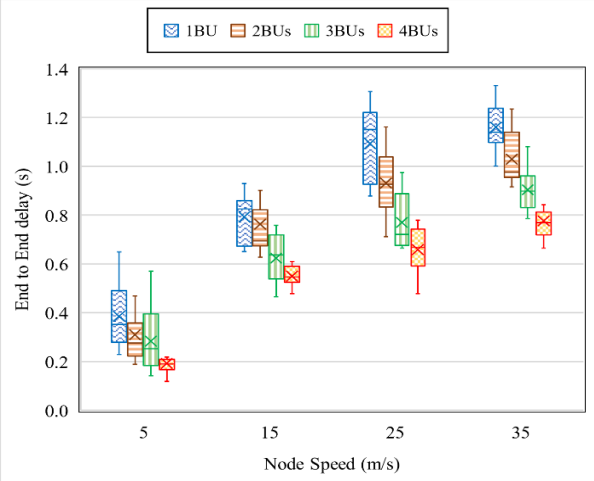

Fig. 10. End-to-end delay performance versus mobility speed for scenarios where total BUs differ.

TABLE III. END-TO-END DELAY VS. NODE'S SPEED BY TOTAL BUS

Measures	Node speed (m/s)	End to End delay (s)			
		1BU	2BUs	3BUs	4BUs
Median	5	0.352	0.275	0.253	0.190
	15	0.826	0.695	0.637	0.546
	25	1.151	0.927	0.721	0.669
	35	1.139	0.976	0.898	0.769
Average	5	0.385	0.310	0.284	0.192
	15	0.793	0.763	0.624	0.550
	25	1.093	0.931	0.770	0.659
	35	1.161	1.029	0.904	0.776

Considering the case of mobility speed of 35 m/s, the median of end-to-end delay for one, two, three, and four BUs are 1.139 s, 0.976 s, 0.898 s and 0.769 s, respectively. The relative average end-to-end delay are 1.161 s, 1.029 s, 0.904 s, and 0.776 s. Thus, the proposed architecture becomes more efficient in terms of end-to-end delay as the number of BUs increases.

B. *Effect of Traffic Load*

This section investigates how variable traffic loads affect network performance, specifically PDR, end-to-end delay, and throughput. The number of connections transmiting data to GCS is altered by adjusting the number of AU senders while keeping the total number of nodes at 50 and the mobility speed of the AUs at 25m/s to simulate various traffic loads. In this assessment, the number of AU senders is 10%, 20%, 30%, and 40%, corresponding to a ratio of 20%, 40%, 60%, and 80% of the total number of FANET nodes.

The PDR and end-to-end delay were used to assess network performance. Fig. 11 depicts the examination of the link between the PDR and the number of senders. According to the data, regardless of the number of senders, increasing the number of BUs correspondingly increases the PDR. When 30 senders were taken into account, the median PDRs for one, two, three, and four BUs were 55.33%, 62.20%, 68.30%, and 71.89%, respectively, while the mean PDRs were 55.75%, 62.17%, 68.21%, and 71.74%. These findings, combined with the analysis data reported in Subsection C1 on the influence of mobility speed in the instance of 20 senders, imply that a greater number of BUs contributes to a higher PDR. To provide a more comprehensive analysis, Table IV below presents detailed data on both the median and average PDR, corresponding to different scenarios with varying numbers of senders. These tables offer a deeper insight into the impact of both the number of senders and BUs on the median and mean PDR

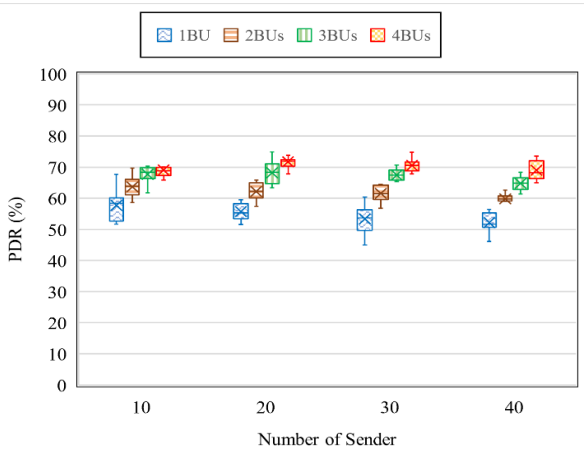

Fig. 11. PDR performance versus number of senders for simulation scenarios where total BUs differ.

TABLE IV. PACKET DELIVERY RATIO VS. NUMBER OF SENDER BY TOTAL BUS

Measures	Number of Sender	Packet Delivery Ratio (%)			
		1BU	2BUs	3BUs	4BUs
Median	10	66.85%	74.58%	78.62%	78.70%
	20	61.69%	67.77%	70.90	76.28%
	30	55.33%	62.20%	68.30%	71.89%
	40	57.78%	61.71%	63.73%	69.14%
Average	10	67.68%	73.91%	79.63%	77.58%
	20	59.13%	67.15%	70.80%	75.63%
	30	55.75%	62.17%	68.21%	71.74%
	40	56.98%	61.96%	64.47%	68.34%

The end-to-end delay was then investigated by altering the number of senders, as shown in Fig. 12. The results show that the end-to-end delay decreases as the number of BUs increases in the majority of scenarios with a given number of senders.

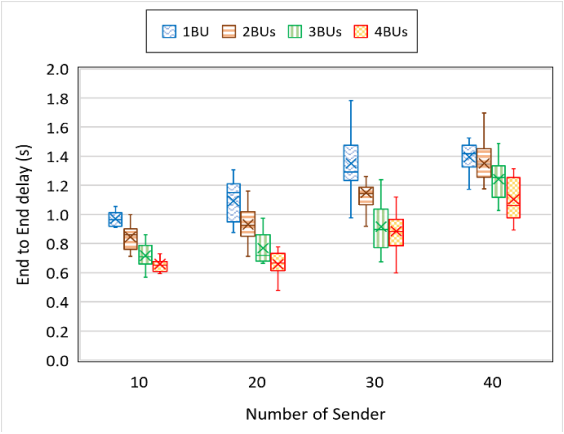

Fig. 12. End-to-end delay performance versus number of senders for scenarios where total BUs differ.

TABLE V. END-TO-END DELAY VS. NUMBER OF SENDER BY TOTAL BUS

Measures	Number of Sender	End to End delay (s)			
		1BU	2BUs	3BUs	4BUs
Median	10	0.964	0.861	0.709	0.653
	20	1.151	0.927	0.721	0.669
	30	1.292	1.142	0.898	0.885
	40	1.416	1.347	1.253	1.063
Average	10	0.971	0.846	0.718	0.660
	20	1.093	0.931	0.770	0.659
	30	1.350	1.149	0.917	0.885
	40	1.395	1.351	1.242	1.104

When the data transmission connection density to GCS is 80% (i.e., 40 senders), for example, the median end-to-end delay drops from 1.416 s to 1.063 s as the number of BUs increases from one to four. Similarly, when the number of BUs increases, the relative average end-to-end delay falls from 1.395 seconds to 1.104 s. These data imply that increasing the number of BUs can improve network end-to-end delay. Furthermore, for a more in-depth analysis, Table V presents a detailed examination of how the number of senders impacts end-to-end delay.

C. *Effect of GCS's Postion*

In this section, the impact of GCS placement on network performance is investigated. For this purpose, a GCS survey was conducted in four distinct sites. These positions are as follows: (1) the Central location at the midpoint of the right edge of the UAV operational area; (2) the North location 350 meters from the midpoint along the right edge; (3) the South location 350 meters from the midpoint in the opposite direction; and (4) a mobile GCS trajectory moving along the right edge at 2 m/s.

Fig. 13 depicts the PDR for various GCS locations. The graph indicates that the PDR increases as the number of BUs grows from one to four for all GCS positions surveyed. When GCSs are located in fixed locations, Central GCS has higher packet transmission efficiency than North and South GCS, as detailed in Table VI. In GCS moving situations, the median PDRs are 53.58%, 63.74%, 67.99%, and 69.04% for 1, 2, 3, and 4 BUs, respectively. The relative average PDRs are 54.87%, 63.08%, 67.63%, and 69.61%, respectively. This implies that increasing the number of BUs can increase network resilience and improve packet delivery from UAVs to GCS.

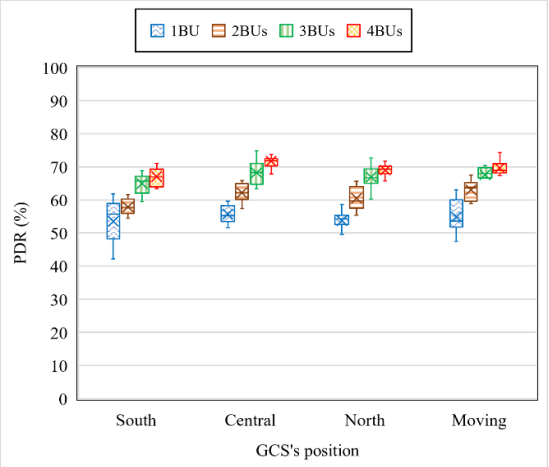

Fig. 13. PDR performance versus GCS's positions for simulation scenarios where total BUs differ.

TABLE VI. PACKET DELIVERY RATIO VS. GCS' POSITION BY TOTAL BUS

Measures	GCS's position	Packet Delivery Ratio (%)			
		1BU	2BUs	3BUs	4BUs
Median	South	55.73%	57.79%	65.78%	66.93%
	Central	55.33%	62.20%	68.30%	71.89%
	North	54.30%	59.68%	66.72%	69.24%
	Moving	53.58%	63.74%	67.99%	69.04%
Average	South	53.55%	57.89%	64.96%	67.05%
	Central	55.75%	62.17%	68.21%	71.74%
	North	53.74%	60.53%	66.92%	69.04%
	Moving	54.87%	63.08%	67.63%	69.61%

For the network throughput, based on the results presented in Fig. 14, it can be observed that the network throughput parameter exhibits an upward trend as the number of BUs increases across all four locations of the GCS.

Study on the delay parameter, the results obtained in Fig. 15 show that the delay decreases gradually when the number of BUs is gradually increased in all cases where the CGS's location is located. The study results depicted in the chart suggest that a central position is an optimal fixed location for the placement of the GCS. Specifically, the findings indicate that the GCS located at the center

position exhibits better latency efficiency compared to the GCS located above, below, or at a distance from the center, with median delays of 1.151, 0.927, 0.721, and 0.669 seconds for the 1BU, 2BUs, 3BUs, and 4BUs cases, and average delays of 1.093 s, 0.931 s, 0.770 s, and 0.569 s, respectively. Furthermore, the results reveal that the latency efficiency of the GCS improves when it moves at a slow speed, compared to the GCS located above, below, or at a distance from the center. Further details and specific data illustrating these findings can be found in Table VII.

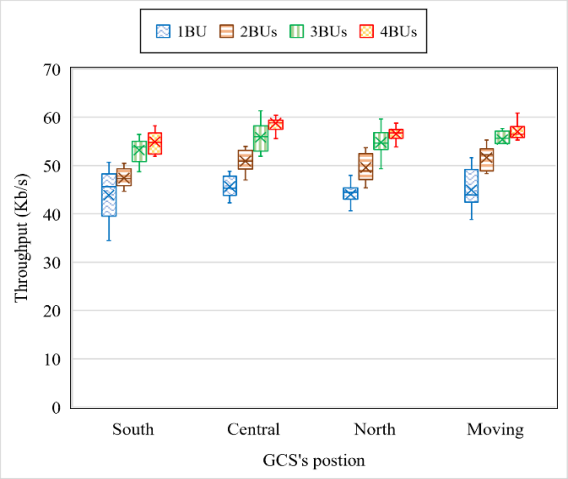

Fig. 14. Throughput performance versus GCS's positions for scenarios where total BUs differ.

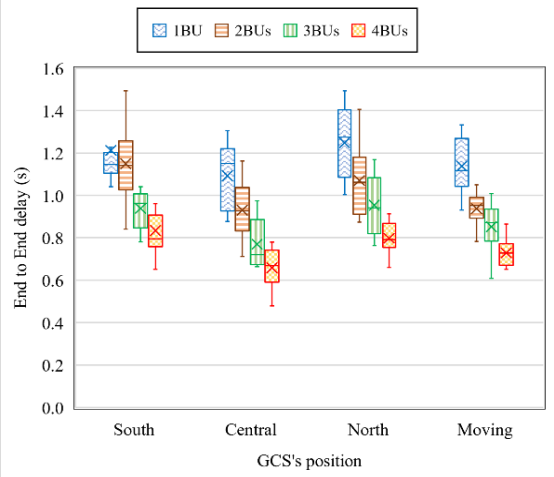

Fig. 15. End-to-end delay performance versus GCS's positions for scenarios where total BUs differ.

TABLE VII. END-TO-END DELAY VS. GCS' POSITION BY TOTAL BUS

Measures	GCS' position	End to End delay (s)			
		1BU	2BUs	3BUs	4BUs
Median	South	1.146	1.142	0.962	0.796
	Central	1.151	0.927	0.721	0.669
	North	1.275	1.063	0.942	0.792
	Moving	1.117	0.952	0.872	0.728
Average	South	1.213	1.150	0.938	0.835
	Central	1.093	0.931	0.770	0.659
	North	1.248	1.071	0.954	0.798
	Moving	1.138	0.938	0.853	0.729

D. *Effect of Network Density*

In order to characterize the influence of network density on the performance of UAV networks, a controlled experimental study is designed by varying the number of UAVs deployed in a fixed area. Specifically, three network scenarios are constructed with 40, 50, and 60 UAVs distributed in a 1500 m^2 area. Increasing the number of UAVs in the same area aims to evaluate the impact of higher network densities on relevant performance metrics. The UAV mobility model is controlled by fixing the UAV speed to 25 m/s across all three scenarios. This ensures that any observable differences in network performance can be attributed to the change in density, rather than varying mobility patterns.

Fig. 16 illustrates the PDR of the proposed architecture in comparison with various network densities. Analysis of the results presented in Fig. 16 reveals that, across all three density cases, the PDR increases with an augment in the number of BUs, and the enhancement decreases as the network density increases. Specifically, corresponding to the number of BUs increasing from one to four, in the case of 40 UAVs, the median PDR 41.2%, 52.85%, 60.47%, 64.11%, in the case of 50 UAVs, the median PDR were 55.33%, 62.20%, 68.30%, 71.89%, and in the case of 60 UAVs, the median PDR was 68.29%, 71.98%, 72.95%, 74.40%.

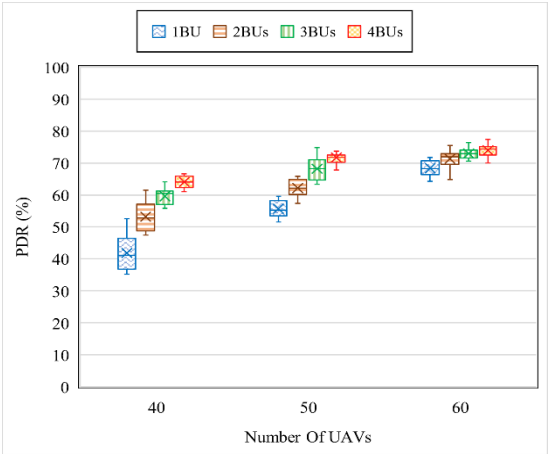

Fig. 16. PDR performance versus network density for scenarios where total BUs differ.

In line with the findings presented in Fig. 17, Table VIII provides specific data on the PDR for the proposed architecture in comparison with various network densities. This table further illustrates the PDR increase with the growing number of BUs across all three density cases, with a diminishing enhancement as network density increases.

The proposed architecture's high PDR is associated with a correlated increase in network throughput. Fig. 17 shows the relationship between network throughput and network density when the number of BUs is 1, 2, 3, and 4, respectively. The presented findings reveal a considerable enhancement in network throughput with an increase in the number of BUs in the sparse network density case (40 UAVs), which aligns with the context of FANETs. The graph data indicates that, as the number of BUs increases

from 1 to 4, the average network throughput improves substantially, with respective values of 33.75 kb/s, 43.30 kb/s, 49.54 kb/s, and 52.53 kb/s.

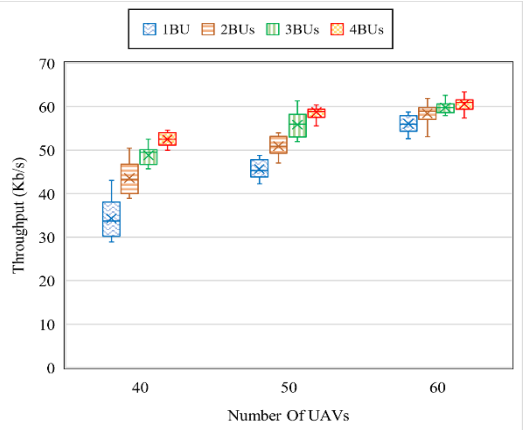

Fig. 17. Throughput performance versus network density for scenarios where total BUs differ.

TABLE VIII. PACKET DELIVERY RATIO VS. NUMBER OF UAV BY TOTAL BUS

Measures	Number of UAV	Packet Delivery Ratio (%)			
		1BU	2BUs	3BUs	4BUs
Median	40	41.20%	52.85%	60.47%	64.11%
	50	55.33%	62.20%	68.30%	71.89%
	60	68.29%	71.98%	72.95%	74.40%
Average	40	41.86%	53.23%	59.59%	64.13%
	50	55.75%	62.17%	68.21%	71.74%
	60	68.43%	71.33%	73.03%	74.01%

Surveying the average throughput over simulation time, the chart in Fig. 18 shows and compares the throughput when using 1BU and 4BUs in the cases of 40 UAVs and 60 UAVs (the case of 50 UAVs is shown in Fig. 8).

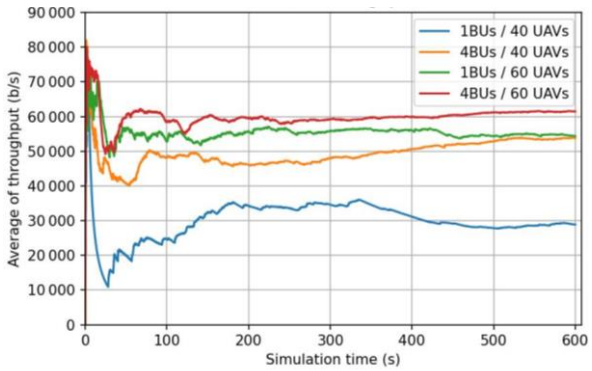

Fig. 18. Throughput performance versus simulation time in case 40 UAV, 60 UAVs with 1BU and 4BUs.

The findings of the study reveal that the network system exhibits instability during the initial simulation period of less than 50 s, leading to notable fluctuations in network throughput. However, as the simulation duration surpasses 50 s, the average throughput reaches a state of stability. Specifically, the average throughput values for scenarios involving 40 UAVs are recorded at 28.86 kb/s and 53.81 kb/s, respectively, for configurations with one and four BUs. Similarly, in scenarios featuring 60 UAVs, the corresponding average throughput values are measured as 54.32 kb/s and 61.48 kb/s for the respective configurations with one and four BUs.

In the conducted survey analyzing end-to-end delay, the graphical representation in Fig. 19 elucidates that, across all three network density scenarios, an increase in the number of BUs from 1 to 4 correlates with a decrease in end-to-end delay. Focusing on the case of a sparse network with 40 UAVs, the median end-to-end delay exhibits the following values with respect to the incremented number of BUs: 1,092 s, 1,058 s, 0.820 s, and 0.693 s. The relative average end-to-end delay are 1.121 s, 1.068 s, 0.826 s, and 0.696 s. Detailed data supporting these findings is presented in Table IX.

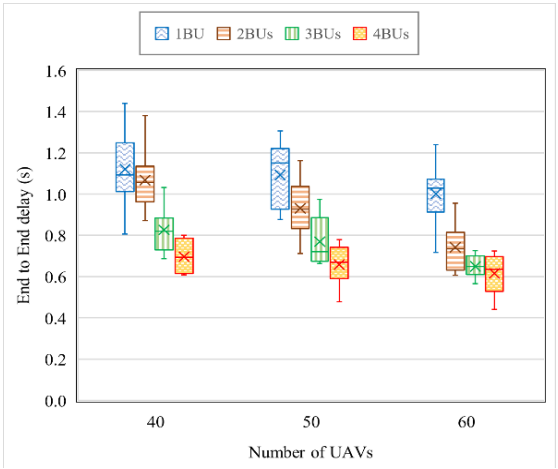

Fig. 19. End-to-end delay performance versus network density for scenarios where total BUs differ.

TABLE IX. END-TO-END DELAY VS. NUMBER OF UAV BY TOTAL BUS

Measures	Number of UAV	End to End delay (s)			
		1BU	2BUs	3BUs	4BUs
Median	40	1.092 s	1.058 s	0.820 s	0.693 s
	50	1.151 s	0.927 s	0.721 s	0.669 s
	60	1.029 s	0.735 s	0.649 s	0.635 s
Average	40	1.121 s	1.068 s	0.826 s	0.696 s
	50	1.093 s	0.931 s	0.770 s	0.659 s
	60	1.002 s	0.742 s	0.650 s	0.616 s

VII. EVALUATION OF PROPOSAL'S ADVANTAGES AND DISADVANTAGES

The main advantage of the proposed architecture is that it is simple to implement but highly effective in terms of packet delivery rate and throughput. The main disadvantage is the need to use several additional UAVs to act as the Backbone Network (BU). However, because the number of BUs is not much, it has a negligible impact on the performance of the network system.

VIII. CONCLUSION

In recent years, the demand for Unmanned Aerial Vehicles (UAVs) in both military and civilian operations had led to a significant increase in research and development activities related to Flying Ad-hoc Network

(FANETs). However, the mobility of UAVs and the implementation of FANETs introduce challenges in achieving efficient end-to-end communications between UAVs with GCS in various applications. An efficient and low-cost hierarchical FANET architecture including two layers was introduced in this paper. The core layer consists of several UAVs flying according to the attached mobility model to form a backbone connecting to the GCS. The access layer includes the remaining UAVs that use the core layer UAVs as gateways to transmit data to the GCS. The proposed architecture's efficiency was assessed on four different scenarios using the AODV routing protocol. Performance metrics were compared in these scenarios with varying number of UAV in the backbone part, specially, 1, 2, 3, and 4 UAVs. The simulation results show that the suggested architecture can reduce average end-to-end time, boost throughput, and increase packet delivery fraction. The increased number of UAVs on the backbone network leads to enhanced performance, however the rise is not linear with the increase in number.

In our vision for future research, we aim to explore a broader spectrum of backbone geometries within FANETs, extending beyond the current focus on line geometry. This expansion will involve experimenting with various backbone configurations and investigating their impact on FANET performance. Furthermore, we plan to design routing protocols based on this proposed solution to further improve FANET routing efficiency.

Conflict of Interest

The authors declare no conflict of interest.

Author Contributions

Tho C. Mai: Conceptualization, conducted the research, original draft writing, editing; Ly T. H. Nguyen, Cuong Q. Nguyen: Simulation, statistics, editing; Le Huu Binh, Tu T. Vo: Conceptualization, supervision, review, throughout the entire writing process; all authors approved the final version of this paper.

References

[1] A. Chriki, H. Touati, H. Snoussi, and F. Kamoun, "FANET: Communication, mobility models and security issues," *Computer Networks*, vol. 163, 106877, 2019.

[2] J. Li, Y. Zhou, and L. Lamont, "Communication architectures and protocols for networking unmanned aerial vehicles," in *Proc. 2013 IEEE Globecom Workshops (GC Wkshps)*, 2013, vol. 3.

[3] O. K. Sahingoz, "Networking models in Flying Ad-hoc Networks (FANETs): Concepts and challenges," *Journal of Intelligent and Robotic Systems: Theory and Applications*, vol. 74, no. 1–2, pp. 513–527, 2014.

[4] M. A. Khan, "Flying ad-hoc networks (FANETs): A review of communication architectures, and routing protocols," in *Proc. International Conference on Latest Trends in Electrical Engineering and Computing Technologies*, 2019, vol. 2.

[5] W. Zafar and B. M. Khan, "Flying ad-hoc networks: Technological and social implications," *IEEE Technology and Society Magazine*, vol. 35, no. 2, pp. 67–74, Jun. 2016.

[6] J. Liu *et al.*, "QMR: Q-learning based Multi-objective optimization Routing protocol for flying ad hoc networks," *Comput. Commun.*, vol. 150, pp. 304–316, 2020.

[7] M. Y. Arafat and S. Moh, "QTAR: A q-learning-based topology-aware routing protocol for flying ad hoc networks," *IEEE Internet Things J*, vol. 9, no. 3, pp. 1985–2000, 2022.

[8] L. A. L. F. D. Costa, R. Kunst, and E. P. D. Freitas, "Q-FANET: Improved q-learning based routing protocol for FANETs," *Computer Networks*, vol. 198, 108379, 2021.

[9] B. Sliwa, C. Schuler, M. Patchou, and C. Wietfeld, "PARRoT: Predictive ad-hoc routing fueled by reinforcement learning and trajectory knowledge," in *Proc. IEEE Vehicular Technology Conference*, 2021.

[10] H. S. Mansour *et al.*, "Cross-layer and energy-aware AODV routing protocol for flying ad-hoc networks," *Sustainability*, vol. 14, no. 15, Aug. 2022.

[11] U. Mohanakrishnan and U. R. D. B. N. R Ashween, "OEE-AODV-optimized energy EEcient routing protocol for reliable data transmission in FANETS OEE-aodv-optimized energy efficient routing protocol for reliable data transmission in FANETS," *Wireless Personal Communications*, vol. 1, 2023.

[12] V. T. Tu, L. H. Binh, P. Dinh, and N. Vu, "Destination sequenced distance vector routing taking into account signal to noise for flying ad hoc network," *Vietnam J Sci Technol*, vol. 61, no. 4, 2023.

[13] D. Y. Kim and J. W. Lee, "Integrated topology management in flying ad hoc networks: Topology construction and adjustment," *IEEE Access*, vol. 6, pp. 61196–61211, 2018.

[14] J. Jailton, T. Carvalho, J. Araújo, and R. Francês, "Relay positioning strategy for traffic data collection of multiple unmanned aerial vehicles using hybrid optimization systems: A FANET-based case study," *Wirel. Commun. Mob. Comput.*, vol. 6, 2017.

[15] T. D. Silva, C. F. E. D. Melo, P. Cumino, D. Rosario, E. Cerqueira, and E. P. Freitas, "STFANET: SDN-based topology Management for flying ad hoc network," *IEEE Access*, vol. 7, pp. 173499–173514, 2019.

[16] A. E. Sara and A. M. Aisha, "Towards enhancement of network communication architectures and routing protocols for FANETs: A survey," in *Proc. 2020 3rd International Conference on Advanced Communication Technologies and Networking (CommNet)*, 2020, pp. 1–10.

[17] J. Jiang and G. Han, "Routing protocols for unmanned aerial vehicles," *IEEE Communications Magazine*, vol. 56, no. 1, pp. 58–63, 2016.

[18] M. Y. Arafat and S. Moh, "Routing protocols for unmanned aerial vehicle networks: A survey," *IEEE Access*, vol. 7, pp. 99694–99720, 2019.

[19] O. S. Oubbati, M. Atiquzzaman, P. Lorenz, M. H. Tareque, and M. S. Hossain, "Routing in flying Ad Hoc networks: Survey, constraints, and future challenge perspectives," *IEEE Access*, vol. 7, pp. 81057–81105, 2019.

[20] D. S. Lakew *et al.*, "Routing in flying ad hoc networks: A comprehensive survey," *IEEE Communications Surveys and Tutorials*, vol. 22, no. 2, pp. 1071–1120, 2020.

[21] Q. Sang, H. Wu, L. Xing, and P. Xie, "Review and comparison of emerging routing protocols in flying ad hoc networks," *Symmetry*, vol. 12, no. 6, pp. 1–24, 2020.

[22] A. F. Güne and I. Abasıkeleş, "Recent topology-based routing approaches in VANETs: A review," *Balkan Journal of Electrical and Computer Engineering*, vol. 11, no. 3, pp. 239–248, 2023.

[23] A. H. Wheeb, R. Nordin, A. A. Samah, M. H. Alsharif, and A. A. Khan, "Topology-based routing protocols and mobility models for flying ad hoc networks: A contemporary review and future research directions," *Drones*, vol. 6, 2023.

[24] L. Mészáros, A. Varga, and M. Kirsche, "INET framework," *Recent Advances in Network Simulation. EAI/Springer Innovations in Communication and Computing*, pp. 55–106, 2019.